biophysica

MDPI

Review

Analysis of Enzyme Conformation Dynamics Using Single-Molecule Förster Resonance Energy Transfer (smFRET)

Mai Huynh and Bhaswati Sengupta *

Department of Chemistry, Pennsylvania State University, University Park, PA 16802, USA; mth38@psu.edu
* Correspondence: bhaswati1487@gmail.com

Abstract: Single-molecule Förster resonance energy transfer (smFRET) enables the deconvolution of various conformational substates of biomolecules. Over the past two decades, it has been widely used to understand the conformational dynamics of enzymes. Commonly, enzymes undergo reversible transitions between active and inactive states in solution. Using smFRET, the details of these transitions and the effect of ligands on these dynamics have been determined. In this mini-review, we discuss the various works focused on the investigation of enzyme conformational dynamics using smFRET.

Keywords: smFRET; enzymes; conformational dynamics

check for updates

Citation: Huynh, M.; Sengupta, B. Analysis of Enzyme Conformation Dynamics Using Single-Molecule Förster Resonance Energy Transfer (smFRET). *Biophysica* **2022**, *2*, 123–134. https://doi.org/10.3390/biophysica2020014

Academic Editor: Attila Borics

Received: 29 April 2022
Accepted: 1 June 2022
Published: 6 June 2022

Publisher's Note: MDPI stays neutral with regard to jurisdictional claims in published maps and institutional affiliations.

Copyright: © 2022 by the authors. Licensee MDPI, Basel, Switzerland. This article is an open access article distributed under the terms and conditions of the Creative Commons Attribution (CC BY) license (https://creativecommons.org/licenses/by/4.0/).

1. Introduction

Fluorescence resonance energy transfer (FRET) emerged as a widely practiced experimental technique toward the end of the past century [1–5]. It is preferentially called Förster resonance energy transfer to lionize Theodor Förster, who first observed the phenomena in 1946 [6]. All the molecules remain in the ground state in the absence of any stimulation. Upon exposure to an external energy source, such as photons, they are excited to higher electronic states. The event of fluorescence stems from the radiative deexcitation of a fluorescent molecule to the ground state. The fluorescence emission of a particular substance (usually termed fluorophore) is characterized by a specific wavelength and intensity. Both the excitation and emission processes have a specific transition dipole moment [7,8]. In order for FRET to happen between two fluorophores, the emission profile of one fluorophore (which acts as a donor) should overlap with the absorption profile of the other (acting as acceptor) to a significant amount. The extent of this overlap is characterized by the overlap integral [7,8]. During an event of FRET, two fluorophores (one energy donor and one energy acceptor) located nearby and having suitably aligned transition dipoles can communicate through a dipole–dipole coupling mechanism to transfer energy, which results in the alteration of the fluorescence signal of each of them compared with when they are not in close proximity (Figure 1A) [7,8]. Owing to the donation, the donor emission intensity goes down and the acceptor emission intensity goes up. The efficiency (E) of this transfer measures the amount of energy transferred per excited donor molecule and shows an inverse proportionality with the sixth power of distance (r) between the fluorophores [9–11]. The distance that allows 50% energy transfer is known as the Förster distance (r_0) [9–11]. This r_0 has a defined value for each donor–acceptor pair, and this value characterizes the specific donor–acceptor pair; a higher r_0 value enables the observation of processes involving a higher distance change. Although FRET operates in a 10–100 Å distance range, its sensitivity depends on a lot of factors, such as the relative orientation of dipoles, the presence of fluorescence quenchers, the overlap integral of the pair (Figure 1B), etc. Because of its distance-dependent nature (Figure 1C), FRET can be utilized to understand an array of biophysical and biochemical processes, such as protein dynamics, drug binding, protein folding, chromatin dynamics, and DNA dynamics [12–16]. When there is a change

in the distance between two moieties in a biomolecule due to intrinsic dynamics or ligand-induced conformational changes, it is reflected in the change in E. From the variations in E, one can calculate the distance change or rate of associated conformational changes.

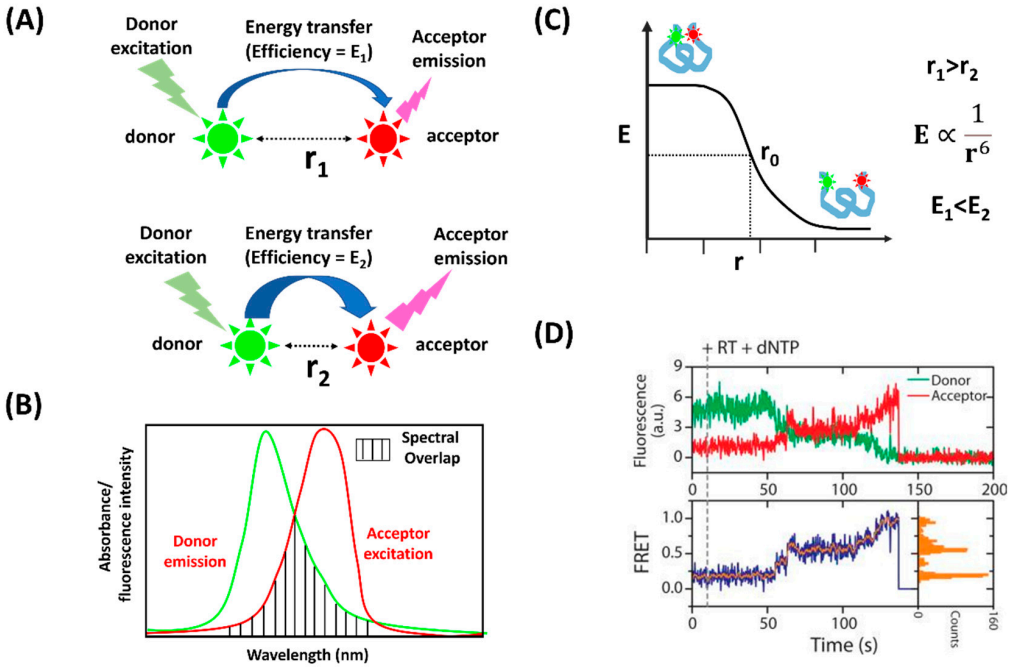

Figure 1. (**A**) Schematic of energy transfer from a donor (green star) to an acceptor (red star). The transfer efficiency depends on the distance (r) between the donor and the acceptor. In the top panel, the donor and the acceptor are further apart than they are in the bottom panel. This results in a much lower value of E for the top panel. (**B**) The spectral overlap (shaded region) between the donor emission and the acceptor absorption. The higher the overlap, the higher the efficiency of energy transfer. (**C**) The dependence of E on distance (r) between two fluorophores labeled on a macromolecule (blue ribbon structure). r_0 denotes the distance at which 50% energy transfer happens. (**D**) Real-time FRET traces from reference [17] with permission. The work involves unzipping of the non-template strand of RNA (labeled with the donor) from the template strand (labeled with the acceptor). Upper panel shows donor (I_D, green) and acceptor (I_a, red) emissions. The bottom panel shows the FRET efficiency (blue) calculated using the equation $E = I_A/(I_D + I_A)$. On the right is the histogram showing population corresponding to the specific value of E.

Although FRET is a very efficient technique to measure inter- and intra-molecular distances, ensemble or solution FRET comes with a few limitations and drawbacks. The first and the most crucial drawback is its inability to deliver precise information about processes that are temporally unsynchronized for different molecules in the solution because of the ensemble averaging of the fluorescence signal. The second point is that there is also a contribution from only donor-labeled or only acceptor-labeled molecules present in the solution because of incomplete labeling, thus making the results erroneous. The third limitation is that ensemble measurements cannot distinguish between subpopulations of different conformational states that are only minutely different from each other. All these drawbacks can be bypassed if one can look at one molecule at a time. Hence, a combination of single-molecule techniques and FRET was highly called for. Two major experimental designs have been adopted by researchers in this regard. One involves recording fluorescence signals from an ultra-dilute solution of dye-labeled biomolecules [18,19], whereas the other uses surface-immobilized dye-labeled molecules for prolonged observation of each molecule [20,21]. In the first case, molecules freely diffusing in and out of the focal volume generate the signal, whereas in the second case, fluorescent pixels are sorted from a recorded movie.

The first report on smFRET came out in 1996 when Ha et al. successfully employed near-field scanning optical microscopy (NSOM) to observe FRET between a tetramethylrhodamine (TMR, donor) and Texas Red (TR, acceptor) couple on 10 and 20 base-pair-long DNA molecules at the single-molecule level [22]. They were able to see distance-dependent FRET changes for different DNA constructs and could obtain information about the possible conformations of DNA from the calculated FRET efficiencies at the single-molecule level. In this mini-review, we discuss all the scientific works focused on conformational dynamics of enzymes using smFRET. Enzymes are one of the most important subclasses of biomolecules, administering many life processes with utmost control and efficiency. The active site of most of the enzymes has at least two conformations: one either facilitates ligand binding or regulates specific processes, and another is inactive conformation. Besides these two, the presence of additional factors is also quite common. The reversible interconversion of these states defines the active site dynamics of the enzyme and is responsible for their specific activity. The timescale of this fluctuation varies from 1 ms to 100 s. Because of the presence of various conformational states with different ligand-binding capabilities and functions, it is practically impossible to scan the active site dynamics with ensemble measurements. This fact justifies the increasing number of reports being published on enzyme conformational dynamics using smFRET. smFRET enables the segregation of different conformational states and the rates of interconversion precisely (Figure 1B). For this purpose, the enzyme must be labeled with one donor and one acceptor dye at the active site, and the distance between these two dyes must be in the range that allows highly efficient energy transfer. Without satisfying the above conditions, the conformational fluctuations cannot be monitored properly.

2. Enzyme Conformational Dynamics

In this mini-review, we tried to put together all the scientific works focused on the investigation of enzymatic conformational dynamics using smFRET (see summary in Table 1). We classified the collection of scientific works into three categories (Figure 2): allosteric regulation type (in which the conformational changes are induced by small-molecule or ligand binding), ligand-independent regulation type (in which the conformational changes are modulated by self-regulation or external factors with no ligand binding required), and feedback regulation type (in which the structural rearrangements are made in response to mismatch binding).

Table 1. List of available reports on the study of enzyme conformational dynamics using smFRET.

Type	Enzyme	References
Allosteric regulation	Staphylococcal nuclease (SNase)	[23]
	T4-lysozyme	[24–26]
	Adenylate kinase (AK)	[27]
	RNA helicase (eIF4A)	[28]
	Telomerase ribonucleoprotein (RNP)	[29,30]
	Phosphoglycerate kinase (PGK)	[31]
	RING E3 ligase	[32]
	ATP synthase	[33]
Ligand-independent regulation type	Hairpin ribozyme	[34,35]
	6-hydroxymethyl-7,8-dihydropterin pyrophosphokinase (HPPK)	[36–38]
	Restriction endonucleases (Ecl18kI and NgoMIV)	[39–41]
	Dengue virus protease (DENV-PR)	[42]
	Sec preprotein translocase	[43]
Feedback regulation type	RNA Polymerases I and II	[44–47]
	CRISPR-associated protein 9 (Cas9)	[48–50]

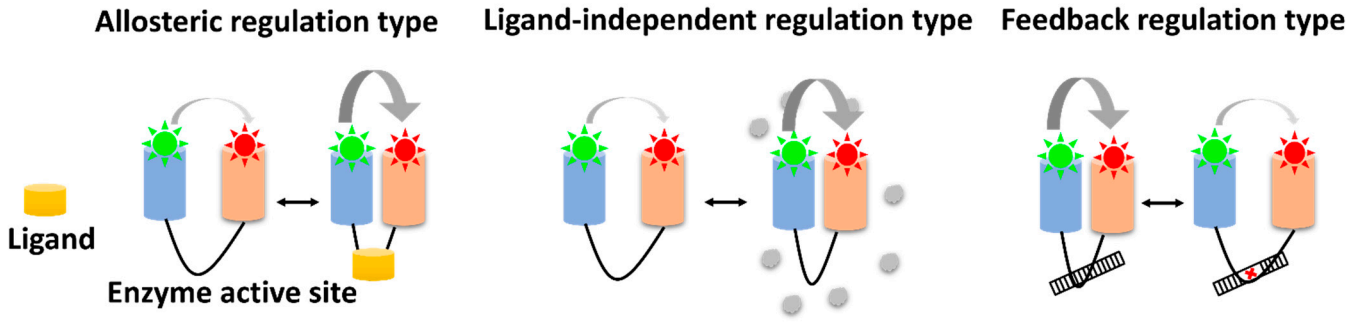

Figure 2. Different mechanisms of enzyme conformational dynamics. Three different categories are discussed in this review: allosteric regulation, ligand-independent regulation, and feedback regulation types. The green symbol represents the donor, and the red symbol denotes the acceptor. The conformational changes are monitored by collecting the changes in the intensities of the two fluorophores under a specific condition of interest.

3. Allosteric Regulation Type

The earliest demonstration of protein as well as enzyme conformational dynamics at the single-molecule level also came from Ha et al. a few years later [23]. Inter- and intra-molecular FRET measurements were performed on TMR (donor)- and Cy5 (acceptor)-labeled surface-immobilized staphylococcal nuclease (SNase) at a 5 ms resolution using a confocal fluorescence setup. SNase is a Ca^{2+}-dependent enzyme that catalyzes the hydrolysis of DNA and RNA into mono- and di-nucleotides. The time-dependent fluctuations of the donor and the acceptor emission showed traces of the anticorrelated donor–acceptor signal that represents FRET. In the presence and absence of an inhibitor (deoxythymidine diphosphate, pTp), the average time constants of the FRET efficiency fluctuations were 41 msec and 133 msec, respectively. These results proved that the conformational dynamics of SNase in the ligand-free and ligand-bound states are significantly different. The successful employment of smFRET in this work paved the way toward a more structured understanding of enzyme conformational dynamics.

Starting in 2003, Peter Lu's group has performed extensive research on the conformational dynamics of T4-lysozyme [24–26]. In the first report, they unveiled the dynamics of the hinge bending motion of the active site of the enzyme [24]. From the results, they could attribute the inhomogeneity in the enzymatic reaction rates to the difference in the time needed for the enzyme molecule to find the binding domain of the substrate. They also found that the subsequent steps had similar rate constants. The presence of different substrate-bound enzyme conformational states was also observed. Later, they also studied the bunching effect of the conformational times and concluded that this effect stems from the convolution of different conformational motions of protein under the effect of the substrate [26].

In 2007, Haw Yang's group reported the smFRET measurements of labeled adenylate kinase (AK) [27]. AK catalyzes the reversible reaction $Mg^{2+}{\cdot}ATP + AMP = Mg^{2+}{\cdot}ADP + ADP$. The ligand-free open conformation and the ligand-bound closed conformation were reported through crystal structures. The Yang group reported the effect of ligand binding on the reversible transition between open and closed states (Figure 3). The timescales of these transitions were calculated as $k_{open} = 120 \pm 40\ s^{-1}$, $k_{close} = 220 \pm 70\ s^{-1}$. Additionally, various conformational substates of the active site of the enzyme were observed through smFRET.

In 2012, Amit Meller's group employed smFRET measurements to study eukaryotic translation initiation [28]. The subject of their study was RNA helicase (eIF4A), which is responsible for unwinding mRNA, thus recruiting ribosomal complexes required for the translation process. Messenger RNA (mRNA) can exist as an RNA/DNA hybrid, which inhibits the binding of the ribosomal complex. By monitoring the changes in the FRET pair between DNA and RNA in the RNA/DNA hybrid, they were able to capture the eIF4AI unwinding activity, which separates RNA from the hybrid and allows for ribosome

docking. They also investigated the relationship between eIF4AI and eIF4H, which has been known to enhance helicase activity. A DNA/RNA hairpin was constructed and labeled with a FRET pair, and by noting its changes in fluorescence intensities, they observed repetitive RNA unwinding activity in the presence of eIF4H in an ATP-dependent manner and an increased eIF4AI/eIF4H complex binding preference for the hairpin loop over single-stranded mRNA.

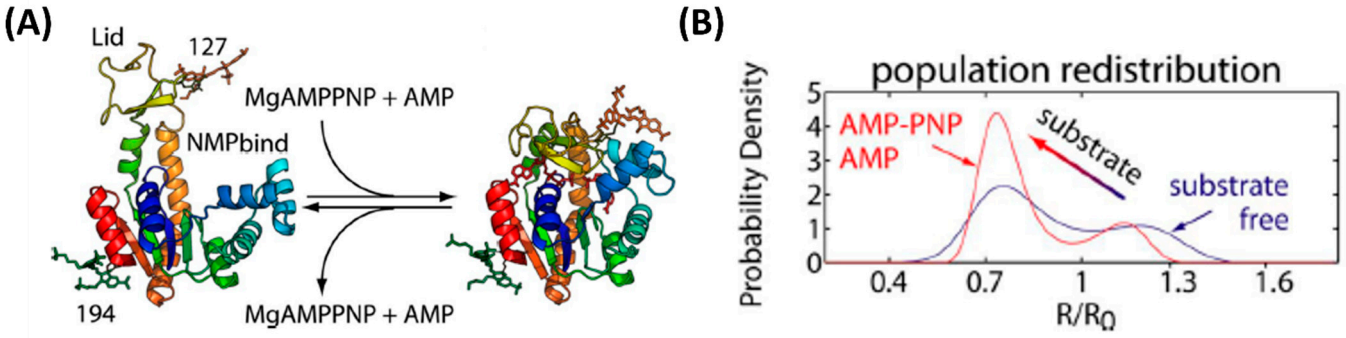

Figure 3. (**A**) Open and closed conformation of AK. The donor and acceptor dyes are labeled at A127 and A194 residues. The open (left) and closed (right) conformations represent the substrate-free and substrate-bound states of AK, respectively. (**B**) The change in R/R_0 reflects the relative change in distance between the donor and acceptor. The population of molecules with a smaller distance (representative of closed conformation) increases significantly upon substrate binding. Figure is adapted from [27]. [Copyright (2007) National Academy of Sciences, U.S.A.].

In 2012, Michael Stone's group from the University of California, Santa Cruz, investigated the conformational changes in the La-domain protein p65, which has been known to regulate telomerase ribonucleoprotein (RNP) assembly [29]. Telomerase RNP is vital for preserving telomere presence and optimal length, whose imperfections can lead to serious cell defects or death. In this research, they explored the interactions between different regions of p65 and telomerase RNA (TER) binding by labeling specific residues within TER with a FRET pair. They found that the C-terminal domain of p65 is required to induce conformation changes in TER, while other regions, despite not directly influencing TER, help stabilize the binding between the p65 CTD and TER. In 2019, a review written by the same group introduced how smFRET measurements provided insights into the structural changes of the human immunodeficiency virus (HIV) reverse transcriptase and telomerase ribonucleoprotein (RNP) enzymes and their potential consequences [30]. In the HIV reverse transcriptase case, the Zhuang group reported that HIV transcriptase possesses contradictory binding structural arrangements for DNA and RNA, and these two binding modes are interchangeable. Additionally, they explored the pathways in which HIV reverse transcriptase is used to search for the correct primer to initiate DNA synthesis [17]. They observed that HIV reverse transcriptase utilizes both DNA sliding and flipping to search for the primer, and the structural arrangement of the viral RNA template can regulate the initiation of the DNA synthesis process by determining the HIV reverse transcriptase binding mode. In the RNP enzyme case, they resolved the interactions between the telomerase essential N-terminus (TEN) domain within the telomerase RNP and either DNA or RNA templates. Therefore, they found that the TEN domain helps in maintaining DNA–RNA hybrids in the telomerase active site not only in eukaryotes but also in yeast and humans.

In 2014, Jorg Fitter's group from Germany used a previously established enzyme system phosphoglycerate kinase (PGK) to study the effects of substrates on the enzyme in ligand-bound complexes [31]. smFRET measurements were utilized to follow the structural changes induced by doubly labeled PGK in the presence of different substrate-binding modes. They found that PGK alone exists predominantly in a compact form, despite a small

population possessing a more expanded conformation, while in the presence of substrate binding, they observed a more compact conformation with an increased population.

In 2020, the Hay group from the UK employed smFRET measurements to study the process of ubiquitination, specifically regarding the mechanism of how RING E3 (a class of E3 ligase) acts on the ubiquitin-bound E2 (conjugating enzyme) complex, thus leading to the transfer of ubiquitin from the complex to the final substrate [32]. On the basis of the fluorescence intensity collected from a FRET pair on ubiquitin-bound E2 complex (E2-Ub), they resolved three conformations of the E2-Ub complex: closed, open, and intermediate. Their results also confirmed that the active conformation is the closed one, where ubiquitin can be deposited onto the substrate. Additionally, they found that the presence of both the UEV (E2-ub binding partner) and the RING domain is required to preserve the closed active conformation of E2-Ub, and the mutations in those regions result in a defective ubiquitination process.

ATP synthases are enzymes that catalyze the process of ATP synthesis from ADP and phosphate. Its working domain is the inner membrane of the mitochondria. Synthases have a large complex structure, which can be described as a rotary nanomotor. The rotary activity of the motor works toward the conversion of electrochemical energy to cellular energy and vice versa. Recently, Sielaff et al. labeled the rotor and stator of F_0-F_1-ATP synthases with a FRET pair to see their relative motion and characterize the ATP-dependent rotation process [33]. They observed a mean rotational frequency of 91 $\pm$ 3 s^{-1} in the presence of 1 mM ATP, which decreased to 42 $\pm$ 3 s^{-1} with 10 μM ATP. With the help of the smFRET-based approach, they were able to resolve the stepwise rotation of F_0-F_1-ATP synthase driven by ATP.

4. Ligand-Independent Regulation Type

smFRET started gaining popularity rapidly around the beginning of the past decade, with an increasing number of articles coming out each year. In 2002, Steven Chu's group published an smFRET-based work on the structural dynamics and function of the hairpin ribozyme, an enzyme that reversibly cleaves its substrate (S) into two products ($3'P$ and $5'P$) [34]. They used part of a hairpin ribozyme (which lacks a four-way junction) and showed the presence of four active (docked) states and one inactive (undocked) state. They also calculated the rates of transitions between different conformational states and proved that these transitions define the rate-determining step of the cleavage reaction. Shortly after this, another article was published by the same group, this time with the hairpin junction intact [35]. This work reported the presence of three distinct states, namely the folded, proximal, and distal states. The folded state converts to the proximal state via a slow, reversible reaction (3 s^{-1}), whereas the proximal to distal transition is fast and reversible (50 s^{-1}). The success of this detailed study of the enzymatic cleavage process can be extended to other ribozymes and other enzymes with complex structural dynamics.

After studying lysozymes, Peter Lu's group focused on HPPK (6-hydroxymethyl-7, 8-dihydropterin pyrophosphokinase) which helps in the biosynthesis of folates by catalyzing the pyrophosphorylation of 6-hydroxymethyl-7,8-dihydropterin (HP), giving rise to 6-hydroxymethyl-7,8-dihydropterin pyrophosphate (HPPP) [36–38]. The catalytic process involves three catalytic cycles. Using an smFRET approach, they showed a coherence of conformational dynamics involved in the catalytic cycles. From the results, they concluded that (i) the product release is the rate-determining step and (ii) the conformational changes do not always lead to product development; they can also be unproductive. Using a correlated smFRET-magnetic tweezers approach, they were able to see a significant restriction of conformational flexibility upon ligand binding.

From 2014 to 2017, Danielis Rutkauskas's lab from Lithuania worked on the interactions between DNA and restriction endonucleases, specifically those leading to DNA looping upon the binding of restriction enzymes [39–41]. In 2014, they started working on Ecl18kI, a well-defined restriction enzyme [39]. Ecl18kI exists in a dimer conformation, and the binding of two dimers on the target DNA strand results in the formation of the active

tetramer complex, which can induce DNA looping on the target DNA strand. By labeling the target DNA strand with a FRET pair, they were able to capture DNA loop formation and kinetics in real-time. From the extracted looping and unlooping kinetics, they observed the productive formation of the active tetramer from two DNA-bound Ecl18kI dimers; however, their complex was short-lived. In 2017, Danielis Rutkauskas's lab employed alternating laser excitation (ALEX) with a 1000 bp DNA template to distinguish two DNA looping conformations induced by Ecl18kI: antiparallel loop and parallel loop [40]. They reported no difference in the lifetimes of DNA looping in either conformation, while the parallel DNA loop formation was much preferred over the antiparallel DNA loop formation. Also in 2017, Danielis Rutkauskas's group published another article on DNA looping induced by another restriction endonuclease, NgoMIV [41]. Unlike Ecl18kI, which only has one DNA binding site, NgoMIV has two DNA binding sites, which can result in more complex DNA-bound NgoMIV conformations. With only one NgoMIV on the target DNA strand, parallel and antiparallel loops are still the only two conformations. However, DNA semi-loops could also form when two NgoMIVs bind to the target DNA strand, in which one binding cleft was bound to the DNA binding site for NgoMIV while the other binding cleft was attached to a nonspecific DNA region. Furthermore, they also reported diverse types of loop formations with different stabilities, in which some loops were more dynamic than the others.

The dengue virus protease (DENV-PR) is a heterodimeric serine protease that plays an active role in the generation of new virus particles in the cell. It has been targeted for drug discovery because of its crucial role in viral infection. In the catalytically active state (closed conformation), the cofactor ($NS2B_{cf}$) wraps around the protease domain ($NS3_{pro}$) to form two pockets S2 and S3 [42]. In the inactive state or the open conformation, the ($NS2B_{cf}$) is disordered [42]. Gotz et al. investigated the presence of different conformational states and their susceptibility to inhibitors [42]. Their results suggested the interconversion of an open and a closed state on a 10 ms timescale. Because of the unstructured nature of ($NS2B_{cf}$) in the open state, this state can adopt different closely related conformations. They also observed that the presence of a competitive inhibitor stabilized the closed state.

In 2021, a collaboration work in Europe utilized the smFRET technique to study the structural rearrangements of Sec preprotein translocase to provide more insights into how a ligand protein can modify itself conformationally and exhibit distinct functions in different environments [43]. The authors reported three conformational states of SecA protein: the open state, the intermediate state, and the closed state. These three conformational states were found to be interchangeable at low concentrations, while the open state was preferred over the two other conformational states at higher concentrations. Therefore, the authors proposed that SecA protein mostly existed in monomers at low concentrations but formed dimers at high concentrations, thus restraining the population of the intermediate and closed conformational states.

5. Feedback Regulation Type

Multiple research projects have been conducted to study the biological activities of polymerase(s) using smFRET over the past decade [44–47]. In 2012, David Millar's group focused on DNA Polymerase I during the DNA replication process [44]. To maintain genomic integrity, DNA Polymerase I must incorporate the correct nucleotide during replication, during which DNA Polymerase I may adopt either the open or closed conformations with DNA. David Millar's group performed an smFRET experiment on a FRET pair between the DNA template and DNA Polymerase I. They successfully presented two previously confirmed conformations (open and closed) and a newly discovered third conformational state (intermediate) for DNA Polymerase I and DNA complexes, all of which were found to be interchangeable during replication. They also found that the closed conformation and a longer DNA Polymerase I resident time were predominant with correct nucleotide insertion, while increased intermediate conformation and fast DNA Polymerase I dissociation were observed with incorrect nucleotide insertion. In 2022, in a review also written by David

Millar, a fourth conformational state was reported with incorrect nucleotide insertion [45]. Therefore, it was suggested that DNA Polymerase I may engage in another pathway to inhibit the insertion of the mismatched nucleotide by altering its interactions with the DNA template, which was confirmed by monitoring doubly labeled DNA Polymerase I in additional smFRET measurements (Figure 4).

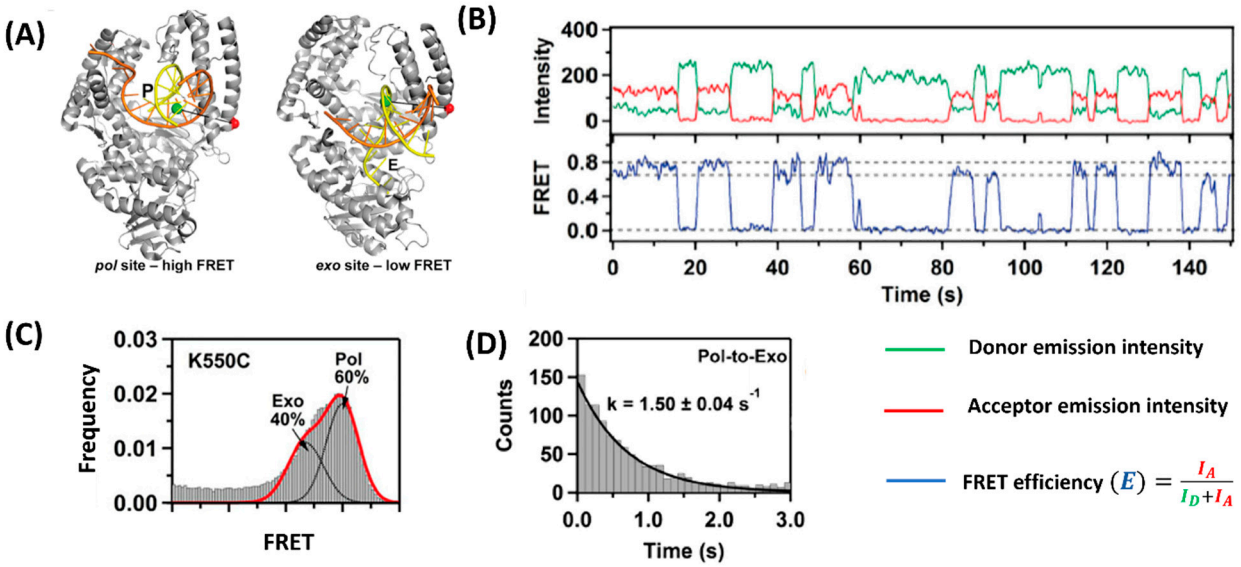

Figure 4. (**A**) Two distinct conformational states detected upon the binding of the Klenow fragment of Pol I. (**B**) The representative trace denoting the changes in the intensities of the donor (green) and the acceptor (red). The FRET efficiency (blue) was extracted. (**C**) The FRET efficiency histogram extracted from the intensities of the donor and the acceptor. Two conformational states were detected and quantified. (**D**) The histogram of the time taken for Pol II to transition from Pol to Exo site. It was fitted (black line) with a single exponential function to obtain the rate constant (k). Figure is adapted from [44] with permission.

In addition to DNA replication, extensive research has been conducted on a different class of polymerase, RNA Polymerase II, during the transcription process [51–53]. In 2014, Gonzalo Cosa's lab from Canada employed smFRET to study the activity of the RNA-dependent hepatitis C virus (HCV) polymerase, which was called non-structural protein 5B (NS5B), in transcription initiation [46]. A DNA–RNA hybrid containing RNA overhang for NS5B binding was constructed with a FRET pair and monitored for its fluorescence fluctuations upon NS5B addition. They reported that the NS5B–RNA complex was more compact at low NSB5 concentrations, while the complex was remarkably more dynamic at high NSB5 concentrations. These changes in the complex behavior were proven to depend on the length of the RNA overhang. Furthermore, they performed similar experiments on different mutations at the entrance and the RNA binding channel of NS5B and found that these mutations led to diminished NS5B–RNA complexes. In 2021, a paper published by Achillefs Kapanidis's group reported structural conformations of RNA Polymerase II and their population changes in different environments [47]. By labeling both the RNA Polymerase II clamp and the active cleft (opposite to the clamp), they were able to resolve three distinct conformational states of RNA Polymerase II, which were the open, partially closed, and closed conformations. It is worth noting that the majority of RNA Polymerase II could switch between different conformation states, and these states could be very long-standing. In this paper, they also found that RNA Polymerase II became less dynamic at increasing concentrations of divalent cations, while increased RNA Polymerase II dynamic motions were observed in the presence of molecular crowding (PEG-8000). An additional study was conducted to study the effects of DNA on the RNA Polymerase II clamp, and

it showed that most RNA Polymerase II in a DNA-rich environment either adopted the closed conformation or possessed a terribly slow transformational dynamic.

Since the invention of Clustered, Regularly Interspaced, Short Palindromic Repeats (CRISPR)-associated (Cas) proteins, Cas9 has quickly gained enormous popularity in the field of genome editing. Since 2014, several papers have been published on the structural conformations and functions of Cas9 protein [48–50,54–60]. In 2018, by doubly labeling Cas9 in an smFRET study, Osuka et al. were able to monitor the activity of different Cas9 domains upon the binding of single-guide RNA (sgRNA) or target DNA [48]. Multiple switching FRET states observed in their smFRET experiments confirmed that Cas9 protein exhibits both flexible and interconvertible conformational states, which were observed in the interactions between a recognition (REC) lobe and a nuclease (NUC) lobe within Cas9. They also found that a more rigid Cas9 was observed upon the addition of sgRNA, while a more dynamic Cas9 was seen upon the addition of the target DNA binding. Another paper from Chunlai Chen's lab focused on the Cas9 complex in the presence of mismatched DNA [49]. Using their smFRET setup, they confirmed three Cas9 fluctuating conformational states, in which the open conformation was predominant, while the closed but active cleavage-competent state of Cas9 was the most minor. With the introduction of double-stranded DNA (dsDNA) mismatches into the Cas9 system, they found that more than four mismatches diminished the intermediate and the active closed states, thus inhibiting Cas9 nuclease activity. In another paper published in the same year, Jizhong Lou's group further investigated the formation and dynamics of an R-loop, which was formed after the binding of gsDNA and dsDNA in the Cas9 protein and was primed to initiate Cas9 nuclease activity [50]. As Cas9 activation requires the recognition of the protospacer-adjacent motif (PAM) on the DNA sequence, the interaction between sgRNA and dsDNA was under investigation for the regions both proximal and distal to the PAM sequence. Interestingly, they observed increased Cas9 cleavage activity in the mismatch of two nucleotides between sgRNA and dsDNA at the PAM distal region, while in general, a higher number of mismatches (>2) between sgDNA and dsDNA resulted in the diminished closed and active Cas9 conformation. At the same time, they also reported a new intermediate state that formed during R-loop formation. This newly found intermediate FRET state became more stable with increasing mismatches between sgDNA and dsDNA. Therefore, the authors hypothesized that the presence of this intermediate state serves as a regulatory mechanism for Cas9 activation.

6. Conclusions

The field of single-molecule spectroscopy is growing each and every day. This comprehensive discussion is just a glimpse of a segment of its use. The use of more than two dyes for site-specific labeling enables the extraction of minuscule structural information; the invention of highly fluorescent dyes helps reduce the noise level; and increasing camera resolution helps visualize ultrafast processes [9,61–67]. Besides these, combining smFRET with other techniques and using theoretical models to analyze the data provides additional information [68–76]. With these upgrades, smFRET serves as one of the most efficient techniques to understand enzyme conformational dynamics and to use this understanding for good.

Author Contributions: Conceptualization, B.S.; Literature Survey: M.H. and B.S.; Writing, M.H. and B.S.; Writing, M.H. and B.S.; Original Figures, B.S.; Review and Editing, B.S. All authors have read and agreed to the published version of the manuscript.

Funding: This research received no external funding.

Institutional Review Board Statement: Not applicable.

Informed Consent Statement: Not applicable.

Data Availability Statement: Not applicable.

Conflicts of Interest: The authors declare no conflict of interest.

References

1. Joo, C.; Balci, H.; Ishitsuka, Y.; Buranachai, C.; Ha, T. Advances in Single-Molecule Fluorescence Methods for Molecular Biology. *Annu. Rev. Biochem.* **2008**, *77*, 51–76. [CrossRef] [PubMed]
2. Lerner, E.; Barth, A.; Hendrix, J.; Ambrose, B.; Birkedal, V.; Blanchard, S.C.; Börner, R.; Sung Chung, H.; Cordes, T.; Craggs, T.D.; et al. FRET-based dynamic structural biology: Challenges, perspectives and an appeal for open-science practices. *eLife* **2021**, *10*, e60416. [CrossRef] [PubMed]
3. Lerner, E.; Cordes, T.; Ingargiola, A.; Alhadid, Y.; Chung, S.; Michalet, X.; Weiss, S. Toward dynamic structural biology: Two decades of single-molecule Förster resonance energy transfer. *Science* **2018**, *359*, eaan1133. [CrossRef]
4. Sasmal, D.K.; Pulido, L.E.; Kasal, S.; Huang, J. Single-molecule fluorescence resonance energy transfer in molecular biology. *Nanoscale* **2016**, *8*, 19928–19944. [CrossRef]
5. Orevi, T.; Lerner, E.; Rahamim, G.; Amir, D.; Haas, E. Ensemble and single-molecule detected time-resolved FRET methods in studies of protein conformations and dynamics. *Methods Mol. Biol.* **2014**, *1076*, 113–169. [CrossRef] [PubMed]
6. Sun, Y.; Wallrabe, H.; Seo, S.-A.; Periasamy, A. FRET microscopy in 2010: The legacy of Theodor Förster on the 100th anniversary of his birth. *ChemPhysChem Eur. J. Chem. Phys. Phys. Chem.* **2011**, *12*, 462–474. [CrossRef]
7. Stryer, L.; Haugland, R.P. Energy transfer: A spectroscopic ruler. *Proc. Natl. Acad. Sci. USA* **1967**, *58*, 719–726. [CrossRef]
8. Selvin, P.R. The renaissance of fluorescence resonance energy transfer. *Nat. Struct. Biol.* **2000**, *7*, 730–734. [CrossRef]
9. Hellenkamp, B.; Schmid, S.; Doroshenko, O.; Opanasyuk, O.; Kühnemuth, R.; Rezaei Adariani, S.; Ambrose, B.; Aznauryan, M.; Barth, A.; Birkedal, V.; et al. Precision and accuracy of single-molecule FRET measurements-a multi-laboratory benchmark study. *Nat. Methods* **2018**, *15*, 669–676. [CrossRef]
10. Kalinin, S.; Peulen, T.; Sindbert, S.; Rothwell, P.J.; Berger, S.; Restle, T.; Goody, R.S.; Gohlke, H.; Seidel, C.A.M. A toolkit and benchmark study for FRET-restrained high-precision structural modeling. *Nat. Methods* **2012**, *9*, 1218–1225. [CrossRef]
11. Dimura, M.; Peulen, T.O.; Hanke, C.A.; Prakash, A.; Gohlke, H.; Seidel, C.A.M. Quantitative FRET studies and integrative modeling unravel the structure and dynamics of biomolecular systems. *Curr. Opin. Struct. Biol.* **2016**, *40*, 163–185. [CrossRef] [PubMed]
12. Larsen, K.P.; Choi, J.; Prabhakar, A.; Puglisi, E.V.; Puglisi, J.D. Relating Structure and Dynamics in RNA Biology. *Cold Spring Harb. Perspect. Biol.* **2019**, *11*, a032474. [CrossRef]
13. Lipman, E.A.; Schuler, B.; Bakajin, O.; Eaton, W.A. Single-molecule measurement of protein folding kinetics. *Science* **2003**, *301*, 1233–1235. [CrossRef] [PubMed]
14. Mazal, H.; Haran, G. Single-molecule FRET methods to study the dynamics of proteins at work. *Curr. Opin. Biomed. Eng.* **2019**, *12*, 8–17. [CrossRef]
15. Michalet, X.; Weiss, S.; Jäger, M. Single-molecule fluorescence studies of protein folding and conformational dynamics. *Chem. Rev.* **2006**, *106*, 1785–1813. [CrossRef]
16. Lee, J.; Crickard, J.B.; Reese, J.C.; Lee, T.-H. Single-molecule FRET method to investigate the dynamics of transcription elongation through the nucleosome by RNA polymerase II. *Methods* **2019**, *159–160*, 51–58. [CrossRef]
17. Liu, S.; Abbondanzieri, E.A.; Rausch, J.W.; Le Grice, S.F.J.; Zhuang, X. Slide into action: Dynamic shuttling of HIV reverse transcriptase on nucleic acid substrates. *Science* **2008**, *322*, 1092–1097. [CrossRef]
18. Deniz, A.A.; Dahan, M.; Grunwell, J.R.; Ha, T.; Faulhaber, A.E.; Chemla, D.S.; Weiss, S.; Schultz, P.G. Single-pair fluorescence resonance energy transfer on freely diffusing molecules: Observation of Förster distance dependence and subpopulations. *Proc. Natl. Acad. Sci. USA* **1999**, *96*, 3670–3675. [CrossRef]
19. Deniz, A.A.; Laurence, T.A.; Beligere, G.S.; Dahan, M.; Martin, A.B.; Chemla, D.S.; Dawson, P.E.; Schultz, P.G.; Weiss, S. Single-molecule protein folding: Diffusion fluorescence resonance energy transfer studies of the denaturation of chymotrypsin inhibitor 2. *Proc. Natl. Acad. Sci. USA* **2000**, *97*, 5179–5184. [CrossRef] [PubMed]
20. Jia, Y.; Talaga, D.S.; Lau, W.L.; Lu, H.S.M.; DeGrado, W.F.; Hochstrasser, R.M. Folding dynamics of single GCN-4 peptides by fluorescence resonant energy transfer confocal microscopy. *Chem. Phys.* **1999**, *247*, 69–83. [CrossRef]
21. Ha, T.; Zhuang, X.; Kim, H.D.; Orr, J.W.; Williamson, J.R.; Chu, S. Ligand-induced conformational changes observed in single RNA molecules. *Proc. Natl. Acad. Sci. USA* **1999**, *96*, 9077–9082. [CrossRef] [PubMed]
22. Ha, T.; Enderle, T.; Ogletree, D.F.; Chemla, D.S.; Selvin, P.R.; Weiss, S. Probing the interaction between two single molecules: Fluorescence resonance energy transfer between a single donor and a single acceptor. *Proc. Natl. Acad. Sci. USA* **1996**, *93*, 6264–6268. [CrossRef] [PubMed]
23. Ha, T.; Ting, A.Y.; Liang, J.; Caldwell, W.B.; Deniz, A.A.; Chemla, D.S.; Schultz, P.G.; Weiss, S. Single-molecule fluorescence spectroscopy of enzyme conformational dynamics and cleavage mechanism. *Proc. Natl. Acad. Sci. USA* **1999**, *96*, 893–898. [CrossRef]
24. Chen, Y.; Hu, D.; Vorpagel, E.; Lu, H.P. Probing Single-Molecule T4 Lysozyme Conformational Dynamics by Intramolecular Fluorescence Energy Transfer. *J. Phys. Chem. B* **2003**, *107*, 7947. [CrossRef]
25. Lu, H.P. Probing single-molecule protein conformational dynamics. *Acc. Chem. Res.* **2005**, *38*, 557–565. [CrossRef]
26. Wang, Y.; Lu, H.P. Bunching effect in single-molecule T4 lysozyme nonequilibrium conformational dynamics under enzymatic reactions. *J. Phys. Chem. B* **2010**, *114*, 6669–6674. [CrossRef] [PubMed]
27. Hanson, J.A.; Duderstadt, K.; Watkins, L.P.; Bhattacharyya, S.; Brokaw, J.; Chu, J.W.; Yang, H. Illuminating the mechanistic roles of enzyme conformational dynamics. *Proc. Natl. Acad. Sci. USA* **2007**, *104*, 18055–18060. [CrossRef] [PubMed]

28. Sun, Y.; Atas, E.; Lindqvist, L.; Sonenberg, N.; Pelletier, J.; Meller, A. The eukaryotic initiation factor eIF4H facilitates loop-binding, repetitive RNA unwinding by the eIF4A DEAD-box helicase. *Nucleic Acids Res.* **2012**, *40*, 6199–6207. [CrossRef] [PubMed]
29. Akiyama, B.M.; Loper, J.; Najarro, K.; Stone, M.D. The C-terminal domain of Tetrahymena thermophila telomerase holoenzyme protein p65 induces multiple structural changes in telomerase RNA. *RNA* **2012**, *18*, 653–660. [CrossRef]
30. Jansson, L.I.; Stone, M.D. Single-Molecule Analysis of Reverse Transcriptase Enzymes. *Cold Spring Harb Perspect. Biol.* **2019**, *11*, a032458. [CrossRef]
31. Gabba, M.; Poblete, S.; Rosenkranz, T.; Katranidis, A.; Kempe, D.; Züchner, T.; Winkler, R.G.; Gompper, G.; Fitter, J. Conformational state distributions and catalytically relevant dynamics of a hinge-bending enzyme studied by single-molecule FRET and a coarse-grained simulation. *Biophys. J.* **2014**, *107*, 1913–1923. [CrossRef] [PubMed]
32. Branigan, E.; Carlos Penedo, J.; Hay, R.T. Ubiquitin transfer by a RING E3 ligase occurs from a closed E2~ubiquitin conformation. *Nat. Commun.* **2020**, *11*, 2846. [CrossRef] [PubMed]
33. Sielaff, H.; Dienerowitz, F.; Dienerowitz, M. Single-molecule FRET combined with electrokinetic trapping reveals real-time enzyme kinetics of individual F-ATP synthases. *Nanoscale* **2022**, *14*, 2327–2336. [CrossRef]
34. Zhuang, X.; Kim, H.; Pereira, M.J.; Babcock, H.P.; Walter, N.G.; Chu, S. Correlating structural dynamics and function in single ribozyme molecules. *Science* **2002**, *296*, 1473–1476. [CrossRef] [PubMed]
35. Tan, E.; Wilson, T.J.; Nahas, M.K.; Clegg, R.M.; Lilley, D.M.; Ha, T. A four-way junction accelerates hairpin ribozyme folding via a discrete intermediate. *Proc. Natl. Acad. Sci. USA* **2003**, *100*, 9308–9313. [CrossRef] [PubMed]
36. He, Y.; Li, Y.; Mukherjee, S.; Wu, Y.; Yan, H.; Lu, H.P. Probing single-molecule enzyme active-site conformational state intermittent coherence. *J. Am. Chem. Soc.* **2011**, *133*, 14389–14395. [CrossRef]
37. He, Y.; Lu, M.; Lu, H.P. Single-molecule photon stamping FRET spectroscopy study of enzymatic conformational dynamics. *Phys. Chem. Chem. Phys.* **2013**, *15*, 770–775. [CrossRef] [PubMed]
38. Guo, Q.; He, Y.; Lu, H.P. Manipulating and probing enzymatic conformational fluctuations and enzyme-substrate interactions by single-molecule FRET-magnetic tweezers microscopy. *Phys. Chem. Chem. Phys.* **2014**, *16*, 13052–13058. [CrossRef]
39. Rutkauskas, D.; Petkelyte, M.; Naujalis, P.; Sasnauskas, G.; Tamulaitis, G.; Zaremba, M.; Siksnys, V. Restriction enzyme Ecl18kI-induced DNA looping dynamics by single-molecule FRET. *J. Phys. Chem. B* **2014**, *118*, 8575–8582. [CrossRef] [PubMed]
40. Tutkus, M.; Marciulionis, T.; Sasnauskas, G.; Rutkauskas, D. DNA-Endonuclease Complex Dynamics by Simultaneous FRET and Fluorophore Intensity in Evanescent Field. *Biophys. J.* **2017**, *112*, 850–858. [CrossRef]
41. Tutkus, M.; Sasnauskas, G.; Rutkauskas, D. Probing the dynamics of restriction endonuclease NgoMIV-DNA interaction by single-molecule FRET. *Biopolymers* **2017**, *107*, e23075. [CrossRef] [PubMed]
42. Götz, C.; Hinze, G.; Gellert, A.; Maus, H.; von Hammerstein, F.; Hammerschmidt, S.J.; Lauth, L.M.; Hellmich, U.A.; Schirmeister, T.; Basché, T. Conformational Dynamics of the Dengue Virus Protease Revealed by Fluorescence Correlation and Single-Molecule FRET Studies. *J. Phys. Chem. B* **2021**, *125*, 6837–6846. [CrossRef] [PubMed]
43. Krishnamurthy, S.; Eleftheriadis, N.; Karathanou, K.; Smit, J.H.; Portaliou, A.G.; Chatzi, K.E.; Karamanou, S.; Bondar, A.N.; Gouridis, G.; Economou, A. A nexus of intrinsic dynamics underlies translocase priming. *Structure* **2021**, *29*, 846–858.e7. [CrossRef]
44. Berezhna, S.Y.; Gill, J.P.; Lamichhane, R.; Millar, D.P. Single-molecule Förster resonance energy transfer reveals an innate fidelity checkpoint in DNA polymerase I. *J. Am. Chem. Soc.* **2012**, *134*, 11261–11268. [CrossRef]
45. Millar, D.P. Conformational Dynamics of DNA Polymerases Revealed at the Single-Molecule Level. *Front. Mol. Biosci.* **2022**, *9*, 826593. [CrossRef] [PubMed]
46. Karam, P.; Powdrill, M.H.; Liu, H.W.; Vasquez, C.; Mah, W.; Bernatchez, J.; Götte, M.; Cosa, G. Dynamics of hepatitis C virus (HCV) RNA-dependent RNA polymerase NS5B in complex with RNA. *J. Biol. Chem.* **2014**, *289*, 14399–14411. [CrossRef]
47. Mazumder, A.; Wang, A.; Uhm, H.; Ebright, R.H.; Kapanidis, A.N. RNA polymerase clamp conformational dynamics: Long-lived states and modulation by crowding, cations, and nonspecific DNA binding. *Nucleic Acids Res.* **2021**, *49*, 2790–2802. [CrossRef]
48. Osuka, S.; Isomura, K.; Kajimoto, S.; Komori, T.; Nishimasu, H.; Shima, T.; Nureki, O.; Uemura, S. Real-time observation of flexible domain movements in CRISPR-Cas9. *EMBO J.* **2018**, *37*, e96941. [CrossRef]
49. Yang, M.; Peng, S.; Sun, R.; Lin, J.; Wang, N.; Chen, C. The Conformational Dynamics of Cas9 Governing DNA Cleavage Are Revealed by Single-Molecule FRET. *Cell Rep.* **2018**, *22*, 372–382. [CrossRef]
50. Zeng, Y.; Cui, Y.; Zhang, Y.; Zhang, Y.; Liang, M.; Chen, H.; Lan, J.; Song, G.; Lou, J. The initiation, propagation and dynamics of CRISPR-SpyCas9 R-loop complex. *Nucleic Acids Res.* **2018**, *46*, 350–361. [CrossRef]
51. Cheung, A.C.M.; Cramer, P. Structural basis of RNA polymerase II backtracking, arrest and reactivation. *Nature* **2011**, *471*, 249–253. [CrossRef] [PubMed]
52. Kettenberger, H.; Armache, K.-J.; Cramer, P. Complete RNA Polymerase II Elongation Complex Structure and Its Interactions with NTP and TFIIS. *Mol. Cell* **2004**, *16*, 955–965. [CrossRef]
53. Komissarova, N.; Kashlev, M. RNA Polymerase Switches between Inactivated and Activated States By Translocating Back and Forth along the DNA and the RNA. *J. Biol. Chem.* **1997**, *272*, 15329–15338. [CrossRef]
54. Nishimasu, H.; Ran, F.A.; Hsu, P.D.; Konermann, S.; Shehata, S.I.; Dohmae, N.; Ishitani, R.; Zhang, F.; Nureki, O. Crystal structure of Cas9 in complex with guide RNA and target DNA. *Cell* **2014**, *156*, 935–949. [CrossRef]
55. Nishimasu, H.; Cong, L.; Yan, W.X.; Ran, F.A.; Zetsche, B.; Li, Y.; Kurabayashi, A.; Ishitani, R.; Zhang, F.; Nureki, O. Crystal Structure of Staphylococcus aureus Cas9. *Cell* **2015**, *162*, 1113–1126. [CrossRef]

56. Szczelkun, M.D.; Tikhomirova, M.S.; Sinkunas, T.; Gasiunas, G.; Karvelis, T.; Pschera, P.; Siksnys, V.; Seidel, R. Direct observation of R-loop formation by single RNA-guided Cas9 and Cascade effector complexes. *Proc. Natl. Acad. Sci. USA* **2014**, *111*, 9798–9803. [CrossRef]
57. Anders, C.; Niewoehner, O.; Duerst, A.; Jinek, M. Structural basis of PAM-dependent target DNA recognition by the Cas9 endonuclease. *Nature* **2014**, *513*, 569–573. [CrossRef] [PubMed]
58. Ban, T.; Zhu, J.K.; Melcher, K.; Xu, H.E. Structural mechanisms of RNA recognition: Sequence-specific and non-specific RNA-binding proteins and the Cas9-RNA-DNA complex. *Cell. Mol. Life Sci.* **2015**, *72*, 1045–1058. [CrossRef]
59. Jiang, F.; Zhou, K.; Ma, L.; Gressel, S.; Doudna, J.A. STRUCTURAL BIOLOGY. A Cas9-guide RNA complex preorganized for target DNA recognition. *Science* **2015**, *348*, 1477–1481. [CrossRef] [PubMed]
60. Josephs, E.A.; Kocak, D.D.; Fitzgibbon, C.J.; McMenemy, J.; Gersbach, C.A.; Marszalek, P.E. Structure and specificity of the RNA-guided endonuclease Cas9 during DNA interrogation, target binding and cleavage. *Nucleic Acids Res.* **2015**, *43*, 8924–8941. [CrossRef]
61. Hohng, S.; Joo, C.; Ha, T. Single-molecule three-color FRET. *Biophys. J.* **2004**, *87*, 1328–1337. [CrossRef] [PubMed]
62. Lee, J.; Lee, S.; Ragunathan, K.; Joo, C.; Ha, T.; Hohng, S. Single-molecule four-color FRET. *Angew. Chem. Int. Ed. Engl.* **2010**, *49*, 9922–9925. [CrossRef] [PubMed]
63. Joo, C.; Ha, T. Imaging and identifying impurities in single-molecule FRET studies. *Cold Spring Harbar Protoc.* **2012**, *2012*, 1109–1112. [CrossRef]
64. Ha, T.; Tinnefeld, P. Photophysics of fluorescent probes for single-molecule biophysics and super-resolution imaging. *Annu. Rev. Phys. Chem.* **2012**, *63*, 595–617. [CrossRef] [PubMed]
65. Zhou, R.; Kunzelmann, S.; Webb, M.R.; Ha, T. Detecting intramolecular conformational dynamics of single molecules in short distance range with subnanometer sensitivity. *Nano Lett.* **2011**, *11*, 5482–5488. [CrossRef] [PubMed]
66. Hohlbein, J.; Craggs, T.D.; Cordes, T. Alternating-laser excitation: Single-molecule FRET and beyond. *Chem. Soc. Rev.* **2014**, *43*, 1156–1171. [CrossRef]
67. Yoo, J.; Louis, J.M.; Gopich, I.V.; Chung, H.S. Three-Color Single-Molecule FRET and Fluorescence Lifetime Analysis of Fast Protein Folding. *J. Phys. Chem. B* **2018**, *122*, 11702–11720. [CrossRef] [PubMed]
68. Liu, Y.; Park, J.; Dahmen, K.A.; Chemla, Y.R.; Ha, T. A comparative study of multivariate and univariate hidden Markov modelings in time-binned single-molecule FRET data analysis. *J. Phys. Chem. B* **2010**, *114*, 5386–5403. [CrossRef]
69. McKinney, S.A.; Joo, C.; Ha, T. Analysis of single-molecule FRET trajectories using hidden Markov modeling. *Biophys. J.* **2006**, *91*, 1941–1951. [CrossRef]
70. Gordon, M.P.; Ha, T.; Selvin, P.R. Single-molecule high-resolution imaging with photobleaching. *Proc. Natl. Acad. Sci. USA* **2004**, *101*, 6462–6465. [CrossRef]
71. Barth, A.; Voith von Voithenberg, L.; Lamb, D.C. Quantitative Single-Molecule Three-Color Förster Resonance Energy Transfer by Photon Distribution Analysis. *J. Phys. Chem. B* **2019**, *123*, 6901–6916. [CrossRef]
72. König, S.L.; Hadzic, M.; Fiorini, E.; Börner, R.; Kowerko, D.; Blanckenhorn, W.U.; Sigel, R.K. BOBA FRET: Bootstrap-based analysis of single-molecule FRET data. *PLoS ONE* **2013**, *8*, e84157. [CrossRef] [PubMed]
73. Pirchi, M.; Tsukanov, R.; Khamis, R.; Tomov, T.E.; Berger, Y.; Khara, D.C.; Volkov, H.; Haran, G.; Nir, E. Photon-by-Photon Hidden Markov Model Analysis for Microsecond Single-Molecule FRET Kinetics. *J. Phys. Chem. B* **2016**, *120*, 13065–13075. [CrossRef]
74. Wilson, H.; Wang, Q. ABEL-FRET: Tether-free single-molecule FRET with hydrodynamic profiling. *Nat. Methods* **2021**, *18*, 816–820. [CrossRef]
75. Kaur, A.; Ellison, M.; Dhakal, S. MASH-FRET: A Simplified Approach for Single-Molecule Multiplexing Using FRET. *Anal. Chem.* **2021**, *93*, 8856–8863. [CrossRef] [PubMed]
76. Hirata, E.; Kiyokawa, E. Future Perspective of Single-Molecule FRET Biosensors and Intravital FRET Microscopy. *Biophys. J.* **2016**, *111*, 1103–1111. [CrossRef] [PubMed]